

**mimed**



Technical University of Munich  
Department of Mechanical Engineering  
Institute of Micro Technology and Medical Device Technology  
Univ.-Prof. Dr. Tim C. Lüth

### Master's Thesis

## Investigation of the Coloring Behavior of Zirconium dioxide ( $ZrO_2$ ) Dental Ceramics by Ink-jet Printing of Metal-ionic Inks

Furkan Öztürk

Matr.-Nr.: 03668338

Supervising  
University Prof. : Univ.-Prof. Dr. Tim C. Lüth

Supervisor: Dipl.-Ing. Dominik Rumschöttel

Issued on: 01.10.2017

Submitted on: 29.03.2018

## **Ehrenwörtliche Erklärung**

Ich erkläre hiermit ehrenwörtlich, dass ich die vorliegende Arbeit selbstständig und ohne Benutzung anderer als der angegebenen Hilfsmittel angefertigt habe; die aus fremden Quellen (einschließlich elektronischer Quellen) direkt oder indirekt übernommenen Gedanken sind ausnahmslos als solche kenntlich gemacht.

Garching bei München, den 29.03.2018

Furkan Öztürk

# **Table of Contents**

<b>Ehrenwörtliche Erklärung</b>	<b>II</b>
<b>1 Introduction</b>	<b>1</b>
<b>2 State of the Research</b>	<b>3</b>
2.1 Structure of the Porous Medium . . . . .	3
2.2 Ink Distribution and Infiltration Time . . . . .	4
2.3 Drop Deployment . . . . .	7
<b>3 State of the Technology</b>	<b>9</b>
<b>4 Review of the State of the Research and Technology</b>	<b>11</b>
<b>5 Assignment</b>	<b>13</b>
<b>6 Expected Advantages and Functions of the Solution</b>	<b>14</b>
<b>7 Solution Structure</b>	<b>15</b>
<b>8 Solution Processes</b>	<b>17</b>
<b>9 Distinctive Features of the Solution</b>	<b>20</b>
<b>10 Experiments</b>	<b>21</b>
10.1 Material Properties . . . . .	21
10.2 Absorption Time . . . . .	22
10.3 Drop Size Selection . . . . .	24
10.4 Proximity . . . . .	26
10.5 Printing Angle . . . . .	31
10.6 Singular Spot Characteristics . . . . .	32
<b>11 Summary and Outlook</b>	<b>39</b>

---

## **Table of Contents**

<b>Bibliography</b>	<b>41</b>
<b>Figure List</b>	<b>43</b>

# 1 Introduction

Only in Germany more than 800 thousand teeth are replaced annually(Hille 2013). The replacement procedure is accomplished with an implantation of the tooth replica to provide the aesthetics and the function of the natural tooth. Ancient Egyptians used tooth shaped ivory to regain the function of the missing teeth. Today the technology has evolved to a point where the dental replacement for a single tooth is an assembly of three parts, which are to be seen in the Figure 1.1. The implant is the part which is screwed to the lower jaw bone (mandible) and it anchors the whole replacement assembly to the chin. The preferred materials used for the implant are titanium in the EU and tantalum in the US. The enhanced osseointegration of the porous implant material surface, biocompatibility of the ceramic interface, which is formed due to the surface oxidation, a Young's Modulus, which is similar to the human bone are the main reasons for titanium and tantalum to be the prime materials for this purpose. The abutment takes on the task of a fitting for the crown and is made of the same material as the implant.



*Figure 1.1: Single tooth replacement*

The crown of the tooth replacement is the part which imitates the visual qualities of the tooth. There are several materials, which a crown can be made of or assembled from. The most popular crown material dominating the market is the Yttria-stabilized zirconia (YSZ) which has a cubic fluorite crystal structure and is going to be referred as zirconia in the frame of this thesis. However, zirconia in its pure form is a plain white material with high translucency. In case of a single tooth replacement, the newly implanted crown would be absurdly white when compared to the neighboring teeth. Even when a full chin dental replacement is conducted, it is abnormal to have a full set of plain white teeth without any shading. This situation makes it a necessity to preprocess the crowns to match the neighboring teeth or another natural shade of choice in case of a fully monolithic replacement. Dentist are using a shade guide seen in the Figure 1.2 for a side-by-side comparison to determine the color and the shade of the teeth. One can observe that there are 4 color groups: A, B, C and D which are referred as orange-brown, yellow, grey-brown and red respectively (VITA 2014). Each of these colors have shades ranging from 1 to 4. Even though the shades are coded with the numbers from 1 to 4 with increments of 0.5, a total analogue shade acquisition is possible. The number 1 represents the shade with the least and 4 with the most saturated tone for each color.



Figure 1.2: Vitapan shadeguide

## **2 State of the Research**

Addressing the shading process of the dental zirconia-based ceramics as a combined procedure of drop generation, dispersion of the ink within the porous material and post sinter generation of the color below the surface of the porous material, it can be said that the quantitative coloring process of the dental crowns is an uncharted area for the scientific researches in the present-day. There have been some research made in the fields concerning the absorption of the liquid by materials presenting a porous inner structure and permeable surface conditions. How the liquid is distributed inside the material, what are the effects of the pore sizes, forms and distributions are investigated by various teams from all around the world for a variety of liquids and porous materials.

### **2.1 Structure of the Porous Medium**

The crystallographic state of zirconia depends on the temperature under atmospheric pressure. Until reaching a temperature of 1170° Celcius, the crystallographic structure shows a monoclinic symmetry. After that temperature the structure can be defined as tetragonal until 2370° C, which afterwards becomes cubic up to the melting point. The volume of the material increases about 4.5% during the transformation from tetragonal to monoclinic phases, which is enough to cause a crack induced failure. This inevitable transformation begins at approximately 950° C while cooling down and the only way to stabilize the tetragonal structure is creating CaO, MgO,  $Y_2O_3$  or  $CeO_2$  oxides inside the structure to keep the tetragonal formation at room temperature, which eliminates the crack initiation and therefore the structural failure of the material parallel to an enhanced toughness (Denry and Kelly 2008).

On a different aspect, some research has been conducted about the effect of the coloring process on the structural strength of the zirconia. In the research of Shah et al., coloring zirconia with cerium acetate mixtures with a maximum ink weight ratio of 5% provided a distinctive shade and did not cause a mechanical disadvantage. However, the ratios above 5% have negative effects on the mechanical properties while not increasing the

shading level significantly. The paper also includes data for a case where the coloring process is conducted using cerium chloride and bismuth chloride. For both cases 1% coloring agent was the limit, if the flexural strength was to be conserved. The low temperature degradation was also observed in the frame of the paper, which did not show any co-dependence with the coloring solution(Shah *et al.* 2008).

## 2.2 Ink Distribution and Infiltration Time

In 2016, Lee *et al.* investigated the absorption behavior of water drops impinging porous stones experimentally and numerically. The investigation includes the phases from spreading to evaporation for a water droplet considering the absorbed amount of the droplet during the depletion and spreading of the humidity within the samples depending on time for three porous materials. Quantitative measurements of the water absorption for the materials are conducted with high-speed imaging and neutron radiography methods during the time range from the impact moment to the end of the spreading phase after absorption. Neutron radiography shows a high resolution quantitative distribution of absorbed water. During the first contact and deposition on the surface, the droplets do not exhibit a wetting behavior. As soon as the droplet acquires its maximum diameter on the surface, it gets fixed and the contact angle with the surface remains constant as long as the droplet is not drained by the stone. The absorption behavior doesn't have the same attributes throughout the whole process. At the beginning, the material shows a contact resistance blocking the absorption, which is associated with the entrapped air beneath the area encapsulated by the borders of the water droplet. In the second phase the encapsulated air finds a way to diffuse away so the capillary flow takes place flawlessly until the total disappearance of the droplet on the surface is observed. The experimental data shows accordance to the phases of the numerical model for water flow inside the unsaturated porous material. The collision velocity has a huge effect on drop spreading on the surface and impregnation, but not so much on the distribution of the water after the initial absorption. The absorption and distribution rates are highly relevant to the capillary structure of the stones (Lee *et al.* 2016).

Pecho *et al.* have conducted experiments to analyse the optical behaviour of dental zirconia and dentin in comparison utilizing Kubelka-Munk theory. The results show that the current zirconia materials alone could not satisfy the luminous transmittance

of the natural dentin so an additive application of masking is required to reach an approximate to the natural tooth(Pecho *et al.* 2015).

The infiltration time of the porous medium was formulated by Markicevic et al. in 2009 as:

$$t_{in} = \kappa \cdot \frac{\mu \cdot r_0^{1.85}}{\sigma \cos(\theta) \phi^{0.38}} \quad (2.1)$$

$t_{in}$  defines the infiltration time and depends on the parameters  $\kappa$ , which is the permeability constant of the medium and  $\mu$  the kinematic viscosity of the fluid. The initial drop radius is symbolized by  $r_0$ .  $\theta$  stands for the initial contact angle after the impact of the droplet on the surface. The  $\sigma$  in the denominator is the surface tension of the liquid. The higher the surface tension is the harder it is for the liquid to wet the surface of the material because of the increased contact angle and hardened impregnation capability. The last dependency of the infiltration time is the  $\phi$  constant for the material, identifying the porosity level of the material (Markicevic *et al.* 2009).

Stratov et al. have provided experimental results regarding the spreading phases of silicon oil droplets utilizing capillary forces over different permeable layers and observing the diameters of the droplets and wetted areas over time. They have divided the depletion into two phases, of which the first one is defined by the time to reach the maximum diameter for the drop base and the second one is identified by the reduction of the drop base while the depletion takes place. The findings of the experiments show that the different oils on the different porous materials with similar porosity and mean pore dimensions showed similar spreading characteristics on a different time scale and the contact angle remained constant throughout the second stage(Starov *et al.* 2002b).

The dispersion behavior of liquid drops inside porous media which are previously saturated with the identical liquid are examined in the work of Starov et al. The study was conducted with both theoretical and experimental perspectives. The spreading of a liquid on a dry solid medium is governed by a power law and it is shown that the same power law applies to the case with saturated medium. The liquid flow within the porous medium is modeled using the Brinkman's equations. The effective lubrication and the liquid exchange between the drop and the porous medium are found to have equal significance through which the drop dispersion equation is generated (Starov *et al.* 2002a).

$$L = L_0(1 + 10(\frac{4}{\pi})^3 \frac{V^3 \gamma}{L_0^{10} \mu} \omega t)^{0.1} \quad (2.2)$$

The formula 2.2 shows the parameters which define the diameter of the covered spot by a deployed drop on the saturated surface of the porous material.  $L_0$  and  $V$  are the measured initial diameter and volume of the drop.  $\omega$  is defined as the effective lubrication coefficient and has to be acquired experimentally for each porous medium and impregnating liquid pair. The  $t$  as the last parameter of the equation stands for the time.

According to Hapgood et al. the properties of the porous medium, such as its porosity, the size and the orientation of the pores and the chemical properties of the surface affect the impregnation and the dispersion behavior of the drops. The Washburn equation is employed by multiple authors to generate a model. These models are grounded on the existence of cylindrical capillaries lying parallel to each other. The Washburn equation describes the behavior of the drops by stating that the wetting is induced by capillary pressure while the viscous dissipation of the flow causes resistance to the dissipation.

The amount of time it takes for a drop to diffuse completely in the porous substrate, until there remains no more liquid on the surface is defined as the drop penetration time, also called as the wicking time.

The fact that the parallel capillary pores assumption not being suitable for direct implementation for powder beds brings about a major disadvantage. To overcome this problem, the Kozeny approach, which utilizes an effective pore size based on the properties of the powder, is widely applied. The 3D velocity components of a Newtonian fluid were measured in the porous medium model under the assumption that the flow is steady, viscous and incompressible. Glass rods with diameters of 3mm were used for building the models of porous media. Two of the velocity components were measured with a laser Doppler anemometer while the continuity equation is integrated to calculate the third component. The main aim was to observe how the viscous drag, inertial flow field and eddy losses in the porous medium affect the flow. The study revealed a laminar and stable flow, which brings along the conclusion that a micromixing of the fluid does not exist. In addition, high values of viscous drag coefficients lead to non-existent inertial flow effects.

Although the vertical and lateral velocity fields are observed to have positive and negative flow fields, the bulk direction flow fields do not have negative velocity fields.

At the top and bottom layers, the vertical flow is found to be absent, based on the fact that the vertical components of the velocities at the top and bottom layers being equal to zero. The fluid advancing in the porous medium via an indirect path should not lead to the conclusion that there exists a fluid mixing, as it is observed to be absent for the examined range of Reynolds numbers.(Hapgood *et al.* 2002)

The diffusion of photons inside the porous medium on which the printing process is carried out, causes the Yule-Nielson effect. This effect is also referred to as optical dot gain and influences the half tone tonality significantly. Thus, it is essential that the Yule-Nielson effect is taken into account, when generating an accurate halftone reflectance model that predicts the halftone color.

The photon diffusion within the porous medium causes the photons to exit the medium from a different spot than where they have entered. Estimating the absorption of light based only on the dot size might be inaccurate due to this phenomena. For instance, when a photon enters the medium from a spot that does not contain ink and leave the medium from a spot that has ink, leading to higher absorption of light. An effective dot size which is greater than the actual dot size is used to compensate this effect.

The halftone tonality is greatly affected by optical dot gain a phenomena caused by the photon diffusion inside the medium. The point spread function (PSF) is one of the ways to model the optical dot gain. The derivation of an appropriate PSF is accomplished through solving the radiative transfer equation, which leads to a PSF in terms of the scattering and absorption coefficients of the medium. This PSF is then used for calculating the average diffusion distance of the photons inside medium. It is shown in the work of Rogers that the Z-sum, which can be expressed explicitly, can be estimated by  $\mu^{-s}$ , where  $\mu$  is the fractional ink coverage and  $s$  has values between 0 and 1. The interrelationship between the PSF approach and the probability approach is proven to be strong. (Rogers 2015)

### 2.3 Drop Deployment

In the book of Eric R Lee, the generation method's parameters and interacting parameters for microdrop generation is comprehensively explained highlighting the possible differences of the outcomes, when different systems are utilized. The available technology for providing a drop on demand printing system rather than continuous jetting is to

be summarized in the next section marking the advantages of each system comparatively.

The first method to consider is the thermal inkjet. If the printing system is considered to be constructed of a nozzle at the bottom to let the generated drops accelerate absolutely vertically to the ground and an ink pool above the nozzle to provide a continuous ink supply during the printing process, a thin heating element can be placed between the nozzle and the ink pool. A high current flow for a fraction of a millisecond through the heating element causes an instantaneous temperature increase in the heating element, which consequently leads to evaporation of the liquid wetting the surface of the heater. The evaporation of the liquid in such a short period means an increase of the volume of the material resting just above the nozzle. This expansion causes the liquid waiting at the tip of the nozzle to be propelled out of the nozzle with the instantaneous pressure pulse. The reaction of the liquid under high temperature is to be taken into consideration.

Piezoelectric ceramics are an elite solution for pulse generation. Under electrical load the piezoelectric material shows elongation in a direction depending on the voltage sign and crystal structure orientation. A tube designed as the nozzle or as the reservoir above the nozzle ejects the fluid out of the nozzle when the diameter of the inner circle becomes smaller under load. Similarly a planer actuator placed above the nozzle feeds the fluid spontaneously in to the nozzle when the electrical loading causes a shear in the direction of the nozzle inside the crystal structure of the piezoceramic. Utilizing the planar actuators is a promising practice for parallel actuator designs for printing purposes.(Lee 2002)

As a third possibility the electromagnetic actuators are a promising solution. An electromagnetic actuator utilizes a persistent magnet as the core material on the flow limiting valve pin and an active coil to create a magnetic field around the core to move it via the generated Lorentz force. Electro magnetic actuation is an affordable solution for the drop deployment problematic, but it comes with its own drawbacks. In comparison to piezoelectric valves there is more heat loss and consequently a lower efficiency. The theoretical drop generation rate is also considerably lower than the one of a piezoelectric valve, due to the high mass and the generated momentum during the movement of the magnetic core in comparison to micro flexion of the piezoelectric ceramic.(Nguyen and Wereley 2002)

### 3 State of the Technology

Even in the most contemporary dental laboratory of today's world, the coloring process is accomplished manually by an experienced dental technologist, who is following the guidelines prepared by the dental ink companies, which explain how a dental crown has to be colored sequentially using different colors on different areas of a single crown summarized in about 20 basic steps for anterior and posterior surfaces of the crowns separately (IDS CAD 2016). The application of the ink on the dental crown with brush strokes takes about 5 minutes for each tooth depending on the manual measurements of the ink application process conducted by a dental technologist from Zirkonzahn for educational purposes.

In the Figure 3.1 you can see a cutout of a lab card showing a section of the anterior teeth with markings. Dentists mark different areas of the crown with different labels referring to the colors from the guide, and send it with an actual photo of the dental area of the patient under warm and cold light to the technician. Therefore, the technician can have a better feeling about the distribution.

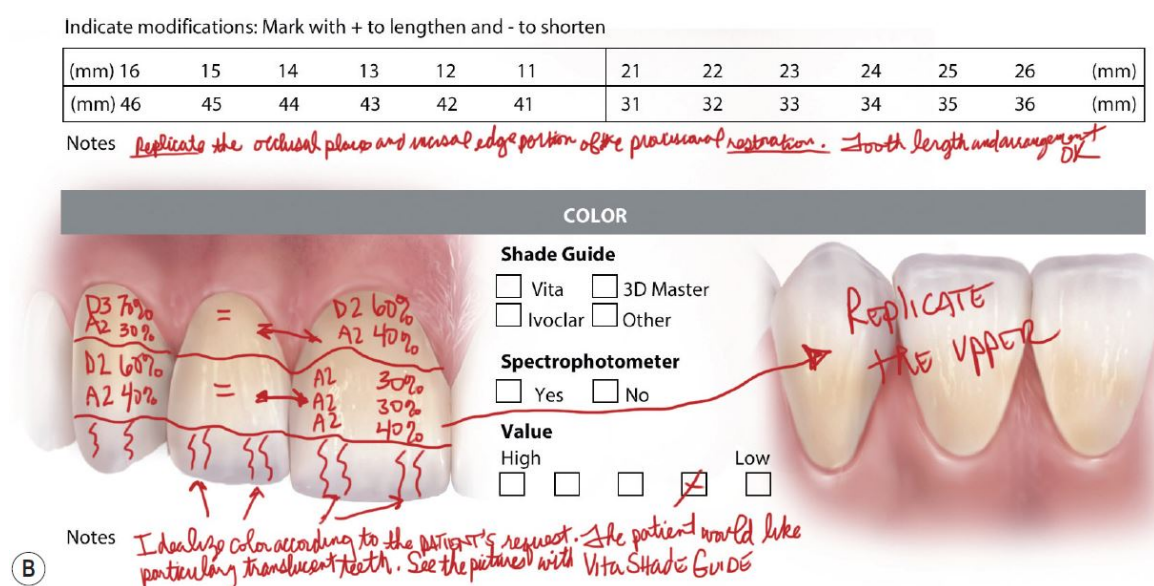


Figure 3.1: Cutout of a lab card (Shapling 2014)

The Figure 3.2 shows the sequential states of the dental crowns after each main process conducted by the dental technologist. First of all, the crowns have to be milled out of cylindrical blank which can provide enough bulk material for about 20 crowns. The milled crowns are colored via variety of brushes using false colored inks to help the dental technician to visually differentiate the colored regions and the inks from each other, which do not possess their final color and have an extremely low contrast so that it is hard process for the human eye to recognize the borders of the different ink applied areas.



*Figure 3.2: Making of dental implants (Zirkonzahn GmbH 2018)*

Afterwards the colored dental crowns are sintered for the ceramic to reach its final strength. The false colors of the inks evaporate at temperatures above 1200°C and the metal-ionic ink becomes more visible providing the zirconia natural tooth like shade which roots from the depths of the ceramic structure. As a final process the crowns are masked and polished.

## 4 Review of the State of the Research and Technology

The second stage ,the coloring process, is the part which this thesis is focused on. The coloring process is a qualitative procedure. The amount of ink to apply on the dents and edges of the crown are described in measures of brush strokes. The literature or the technical documentation does not provide a quantitative approach about the required amount of ink. In Figure 4.1 one can observe how cumbersome it is to accomplish the full colorization of a crown. More importantly, if the batch size is large an important problem surfaces. The sequential teeth have to comply with the natural ones already present in the application area or the ones colored before. The shading tolerances cannot be allowed to be too high, because of the uncommon irregularity of the teeth colors this situation would cause.



*Figure 4.1: False colored crowns after manual brushing (Zirkonzahn GmbH 2018)*

There are already devices to check the generated shade as a quality control measure. The proactive measure to control the shade to be generated is premixing the coloring agent with the brightener at the factory to guarantee that the zirconia will have the predefined color after the sinter if the zirconia is soaked in to the ink or the ink is applied on the surface until saturation is reached. For the printing process the amount of ink required for each shade, the time of depletion of the micro drops from the surface of the zirconia in the the porous structure and the size of the generated spot as well as the

distribution of the ink depending on the radial distance from the center of the spot is of high interest.

## 5 Assignment

In frame of this thesis a process is to be developed for generation of the dental color shades using an inkjet printer. The mechanic aspects of responsible for the movement are not included to the project. A stepper motor driven system responsible for the coordinated movement of the axes controlled by a SmoothieBoard v2-mini is provided by the project partner Bredent GmbH. The specifications of the printing system, like a single drop volume or the max printing distance and angle are to be determined.

Afterwards, an adequate droplet generator is to be selected. The diameter of the nozzle is as important as the driver technology generating the droplets, which has a direct effect on the optical resolution of the printed pattern. With piezoelectric droplet generators, smaller and faster drops are possible but electromagnetic ones are cheaper. The quantitative coloring behavior depending on the absorption characteristics of the dental ceramic is an unknown to the state of the research and the technology. The shades of the dental colors are to be brought about using the main colors with the highest saturation level and a brightener, which is a water based diluter with an identical composition to the inks, except lacking the metal-ionic coloring agent. The proportions of the ink and the diluter is not the only parameter affecting the shade of the generated color, but also the application sequence can have a significant effect on the optical perception. Since the translucency of the dental zirconia effects the level of color reflection, the depth of the colored section can have an undeniable effect on the natural look of the dental crown.

At last, the generated shades are to be verified with the existing color standards. The receipt for each single shade generation has to be prepared. The deployed droplets are not expected to fly and settle on the contact point drying on the surface, but are expected to be absorbed and spread inside the porous material. This nature of the interaction between the ink in its fluid form and porous zirconia defines the system as a nonlinear three dimensional fluid dynamics problem. A model is to be generated taking the every compensational aspect of the nonlinear ink behavior, in order to achieve a point accurate color acquisition.

## **6 Expected Advantages and Functions of the Solution**

One of the most important advantages is quantification of the coloring process followed by the printing process. Until this day, the crown coloring process is made by dental technologists all around the world. In other words, all of the dental replacements are partially handcrafted. In the market, hand crafted is another word for made by a craftsman, specifically for the unique owner of the product. Just as any other product on the market, the word handcrafted has a prominent effect on the price tag of the item. The word handcrafted also means the product has some tiny error, a nuance special for each unique sample. If the object of interest is a decor for the home of the consumer, it is one of the most welcome properties. However, if the object of interest is an implant, which is to be carried all the time on the consumer's body as a part of the it, the property everyone is looking for is perfection. A perfect shape, color, consistency and harmony is a standard to evaluate the quality of the work done by the dentist and of course involving the dental technologist. The quantification of the coloring process is the most important advantage of the solution when it is considered looking from this aspect. Thus, the error can be terminated and the quality deviation can be limited to an acceptable variance.

Another aspect to consider is the ink costs. Each of the ink bottles are labeled with the same price tag by the manufacturer. However, not all of the ink bottles contain a material worth the same value actually. The shades of the colors ranging from 1 to 3.5 are only diluted versions of the bottle with the shade 4.0. Buying the most concentrated tone and diluting it is here an economical solution, as it is in every other section of the industry. Also, the whole spectrum of shades can be obtained with only 4 ink bottles and a brightener by halftone printing. The required purchase variety, transportation costs, and the space requirement are all reduced with the usage of only the most saturated shades.

## 7 Solution Structure

The structural concept is based on the utilization of a 5-axis printing system. A basic microcontroller designed for the automation of the router systems is connected to stepper motors and encoders to control the coordinated printing processes. 4 base colors with the highest saturation levels (A, B, C and D4) are to be used with the brightener to color the dental zirconia, instead of 17 bottles consisting of 16 predefined shades plus the brightener. The amount of the brightener defines the shade of the color. Therefore, the space requirement of the machine is reduced. The inks and the brightener are continuously fed into a rotary distribution valve and are in their neutral status not flowing in any direction. As soon as the rotary valve opens the gate of any incoming pipe, the flow is permitted to the droplet ejector.

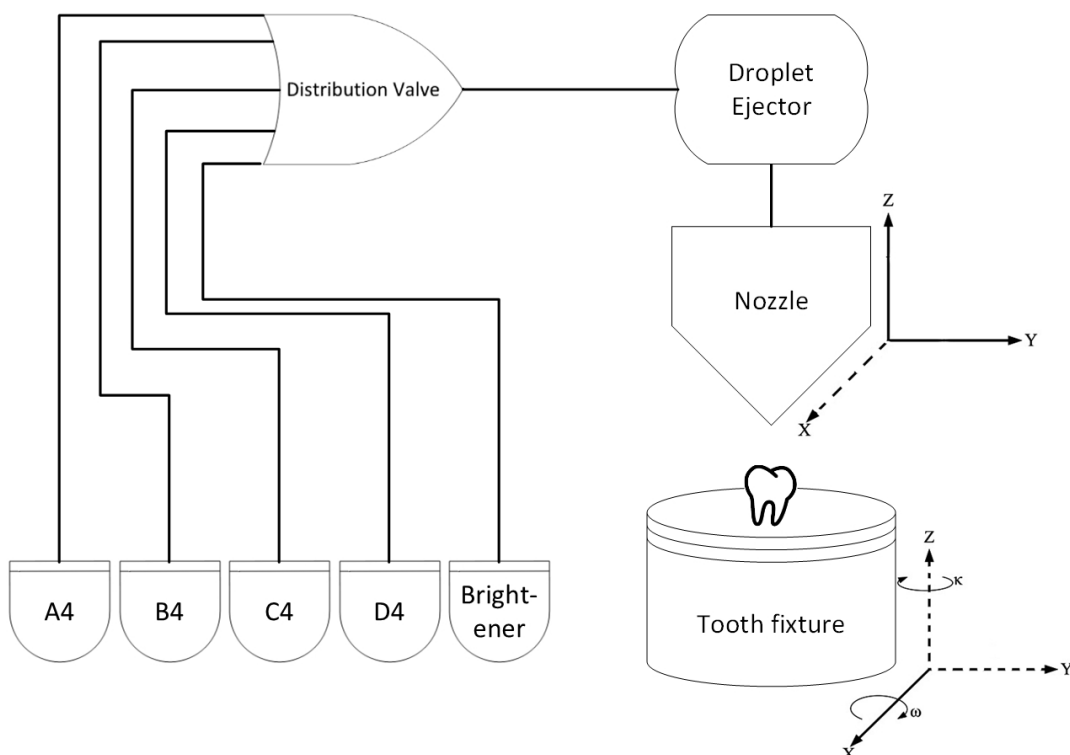


Figure 7.1: Solution Structure

A serial communication between the controller and the rotary valve arranges the position of the rotary valve and the duration to hold on in that position. The required mixture is dosed and pulled by the droplet ejector and deployed through the nozzle, driven by the pressure difference between the ink bottles at the beginning of the cycle and the atmosphere. A 3-axis table and the 2-axis nozzle holder are responsible for the coordination of the flying drops and the point on the surface of the dental crown where the drops need to land during the printing process.

## 8 Solution Processes

The process concept is realized in three stages. Each stage depends on the previous one and cannot be proceeded to, before the previous one is completed.

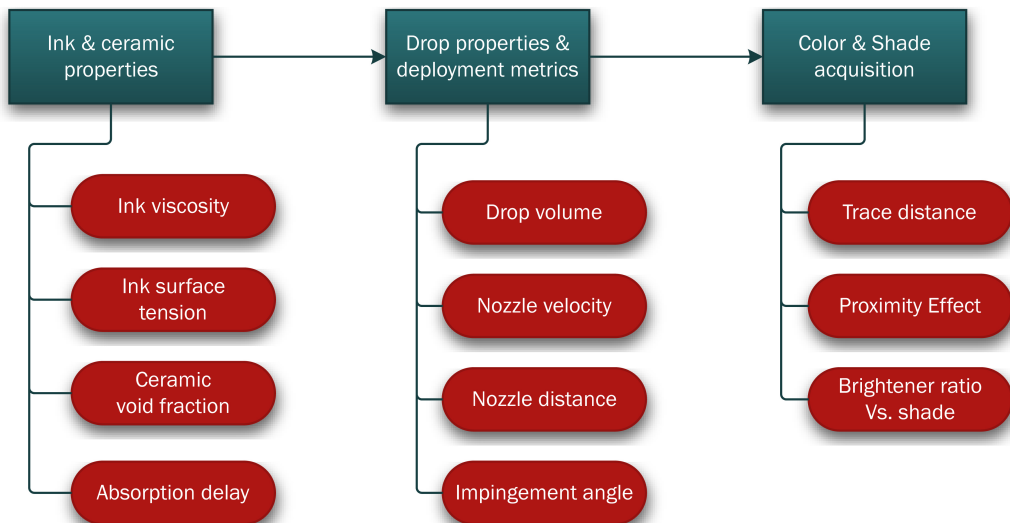


Figure 8.1: Solution Processes

First stage is finding the ink and ceramic properties, such as ink viscosity and surface tension, ceramic void fraction and ink absorption time. Depending on these experimentally acquired parameters the equations 2.1 and 2.2 can be utilized in the progress of the model generation for the drop deployment algorithm for an arbitrary pattern to be printed on the zirconia material.

Second stage is planned to help determine the parameters defining the printing system. It basically focuses on the settlement of drop properties and deployment metrics, which consist of drop volume, nozzle escape velocity of the drops, the optimal distance between the nozzle and zirconia surface and the angle between the drop projectile and the surface. The drop volume has to be determined as soon as possible, because

it directly affects the selection of the actuator which is to be used as the drop ejector. Selection of a larger drop size means a shorter printing time. However it also means that the resolution is supposed to become lower. Due to the absorption characteristics of the zirconia material, a critical drop size is expected to cause a significant effect on the diameter of a painted spot. In other words, deploying the same amount of ink on the same spot using drops with a volume of smaller than 5 nL could give the same printed spot diameter. In comparison to the aforementioned drop volumes, using 10 or 20 nL drops to apply the same amount of ink on a single point could result with an unexpectedly larger spot size with lower central intensity. This critical drop size has to be determined, in order to proceed to the rest of the experiments.

The projectile velocity of the drops is one of the most important parameters affecting the printing system on a temporal basis and also the spreading characteristics of the ink within the porous medium. It is known that for Weber numbers higher than 50, the drops are expected to splash upon the impact with the surface (Clarke *et al.* 2002).

$$We = \frac{\rho r v^2}{\gamma} \quad (8.1)$$

The maximum distance of the nozzle to the zirconia surface has to be limited. The projectile of the droplets are not perfectly identical. There is a deviation of the impact point, because of the factors like a slight change of the nozzle escape angle of an arbitrary droplet or drag caused by the spontaneous fluctuation of the air flow inside the printing chamber. The longer the fly distance of the droplets are, the less accurately they will meet the same point. So the deployment distance for the droplets should be as short as possible. However on the other side the geometry of the crown creates the second boundary of the problematic. The concave structures on the upper side of the teeth carrying out the chewing function pose a collision danger with the nozzle. This is a situation where the printing angle is also influential.

The aspects to be considered under the third stage are employed to conduct an experimental approach to color and shade acquisition. In order to arrive there some parameters have to be determined. Firstly the appropriate trace distance for the selected drop size is to be concluded, depending on the experiment with varying trace distances, which is the distance between two sequential lines on the printed surface. The proximity effect is the second nonlinear parameter affecting the print resolution and color distribution, which refers to how the proximity of two colored areas affect the shade of the uncolored

area in between. Finally the dependency of the shade on the brightener ratio is to be determined. For a liquid inside a bottle it is very easy to come to a final conclusion. However, the porous translucent medium has a huge influence on the perceived shade, because of the reflections from various depths of the material and photons following diverse paths through the sintered zirconia to the eye of the observer.

All of the aforementioned tasks are to be carried out so at the end a model can be generated. This model has to work as an algorithm to calculate the input pattern for a desired arbitrary shade map of a dental crown geometry. The coloring behavior on the printed sample has to be compared with the virtually printed geometrical model.

## **9 Distinctive Features of the Solution**

The most contemporary dental laboratory of today still has to do the coloring process manually. A dental technologist uses brushes to apply tens of bottles of ink shades to the dental crowns one by one following the procedures described by dental zirconia ink manufacturers. Coloring each tooth takes about 5 minutes and about 100 precise brush strokes. This is a process which requires a high patience and repeatability. This project is the first automated printing approach in dental coloring sector. With the automation of the procedure many advantages are expected. The accuracy of shade acquisition is to be guaranteed because of the quantified and digitalized coloring procedure. The variation between the sequential teeth are to be minimized. Shorter lead times can be realized upon the optimization of the printing method, which is to be accompanied by lower costs due to the automation and shortened process time.

Another novelty of the project is the discontinuation of the requirement for a bottle for every single shade of each color. The lighter shade of each color are only bottle mixtures of the brightening fluid and the darkest shade of that color by the manufacturer. The mixtures do not posses a linear ratio for the contained ink and brightener depending on the color shade. The mixture is prepared considering the end shade to be acquired on the zirconia. This project makes it possible for the first time to generate the shades using the darkest base colors and a brightener, thanks to the digitalization of the coloring procedure.

## 10 Experiments

Before moving on to the experiments I want to show you the 5 axis printing system prototype provided by Bredent GmbH. for conduction of the experiments. It utilizes a single nozzle print head with a piezoelectric valve to generate the droplets. Ink selection, positioning and drop generation commands are given with a G-Code.

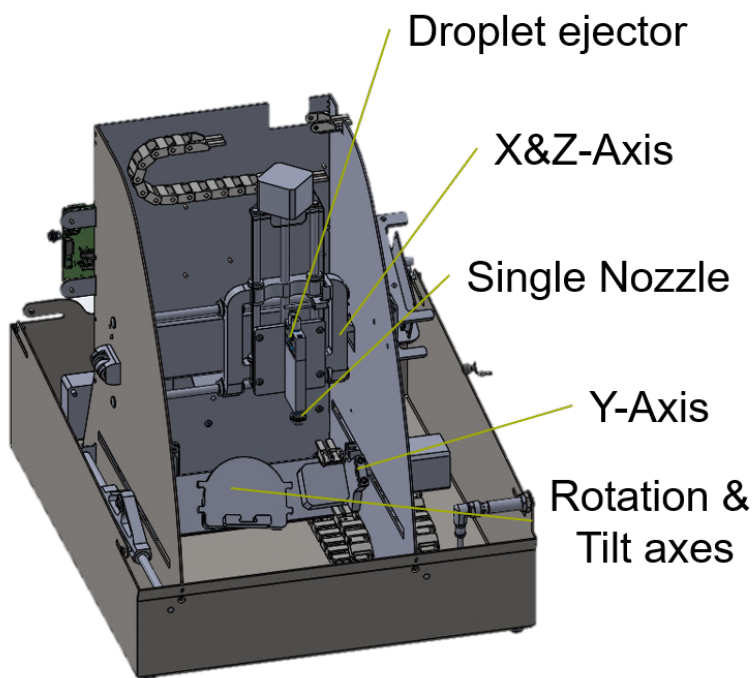


Figure 10.1: 5 axis printer design for dental ink (Matthias Leininger, Bredent GmbH)

### 10.1 Material Properties

For a dental technician it is completely trivial how viscous the ink is but for an automated printing process the quantization of the properties is highly important. In the first

experiment, the properties of the coloring agents A1, A2 and A3.5 are determined and compared to those of water. The inks have a similar density to water, but with increasing coloring agent the surface tension gets lower and the viscosity gets 3 times higher when compared to water. Also, a porosity measurement for the zirconia is conducted, which revealed a 43 percent void fraction. The raw volumetric porosity measurements are 43.09, 43.00 and 43.70. The consistency of the results is also a sign for randomly close packed zirconia powder during the manufacturing procedure. Otherwise the irregular packing would inhibit the fluid drainage and cause macro voids inside the porous material after the dissipation of the impregnating liquid, which would also lead to porosity measurements with a significantly large standard deviation.

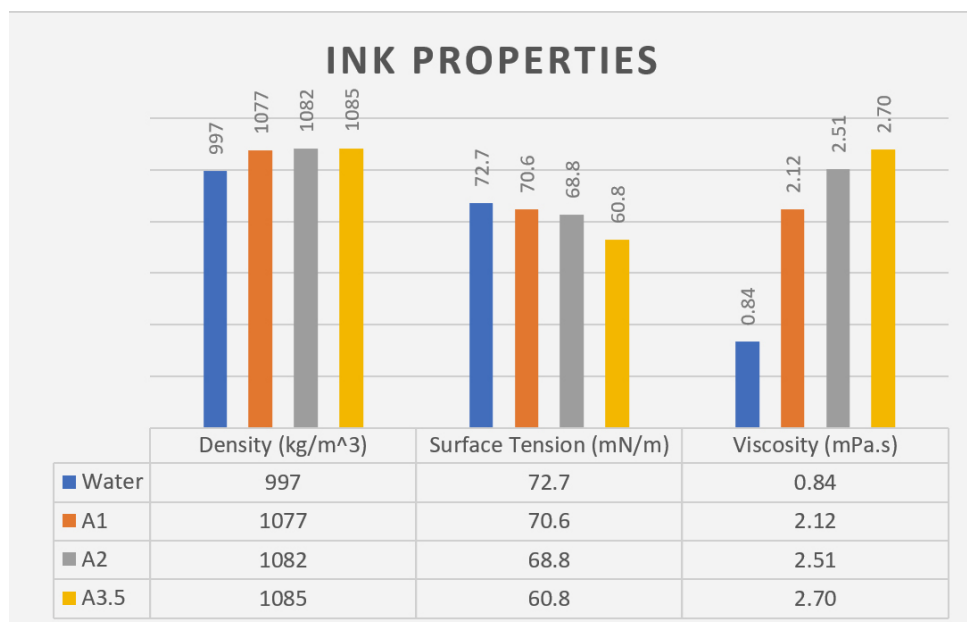


Figure 10.2: Ink Properties

The most important outcome of this experiment is high values of viscosity observed for the inks, in comparison to water. This situation provides numerous advantages for the drop generation part of the process. The higher viscosity of the ink helps reduce the occurrence of the satellite drops.

## 10.2 Absorption Time

The second experiment is about the absorption time of the droplets which limits the printing time. Before the first drop is absorbed, a second drop should not land on the

same spot. This would lead to accumulation of the liquid on the surface and eventually they would flow in the direction of the first drop because of the surface which is already wetted. The target accuracy of the drop deployment system would lose all of its importance. The resolution would be also sacrificed alongside the target accuracy, due to the accumulated liquid on the surface. The absorption time is formulated by Markicevic et al. as in equation 2.1.

Depending on the Eötvös rule, the surface tension of any Newtonian liquid declines with climbing temperature values. For water the formula is generated as:

$$\gamma = 0.07275 \cdot (1 - 0.002 \cdot (T - 291)) \quad (10.1)$$

Arrhenius-Andrade-Relation defines the viscosity of any Newtonian fluid depending on the temperature in the equation 10.2.

$$\eta = \eta_0 \cdot \exp\left(\frac{E_A}{R \cdot T}\right) \quad (10.2)$$

The exponential reduction of the viscosity versus the proportional decrease of the surface tension would be expected to result with a cumulative decrease of the absorption time with climbing temperatures.

Single drops with a volume of 100 nL are deployed on the sawn and milled surfaces. The time between the landing and complete absorption was measured 4 times for each surface structure at the temperatures 20° C, 30° C, 40° C, 60° C and 80° C.

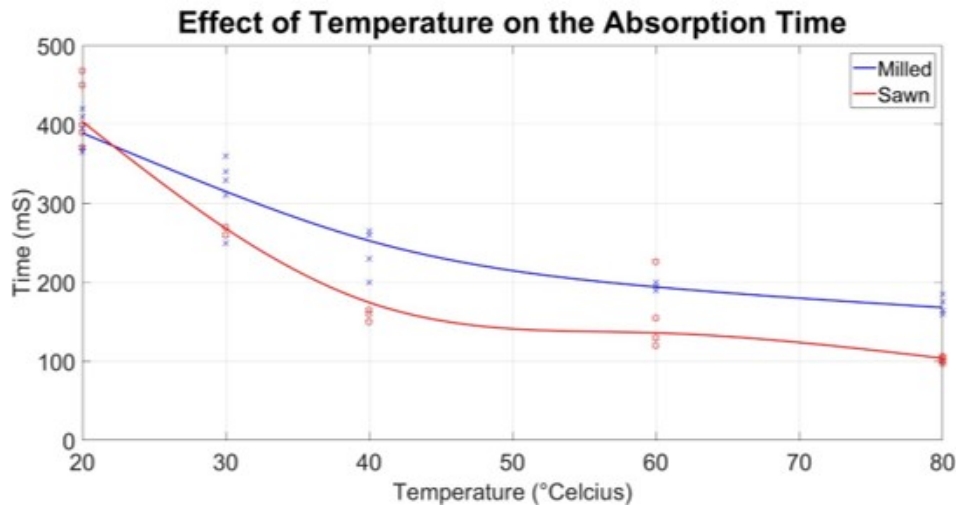


Figure 10.3: Effect of heat on the absorption time

Analyzing the collected measurements, it can be concluded that a 60° C increase of the zirconia plate leads to about 50% decline of the absorption time. Thus the printing time also gets reduced to half of the duration it would take under room temperature.

### 10.3 Drop Size Selection

The purpose of the third experiment is deciding for an adequate drop size. A larger drop size results in shorter print duration. However they also tend to expand the spot area more compared to the smaller drops, even though the porous material is not close to being saturated, which is a serious problem for the resolution. Depending on the drop size, the drop generation method is to be selected.

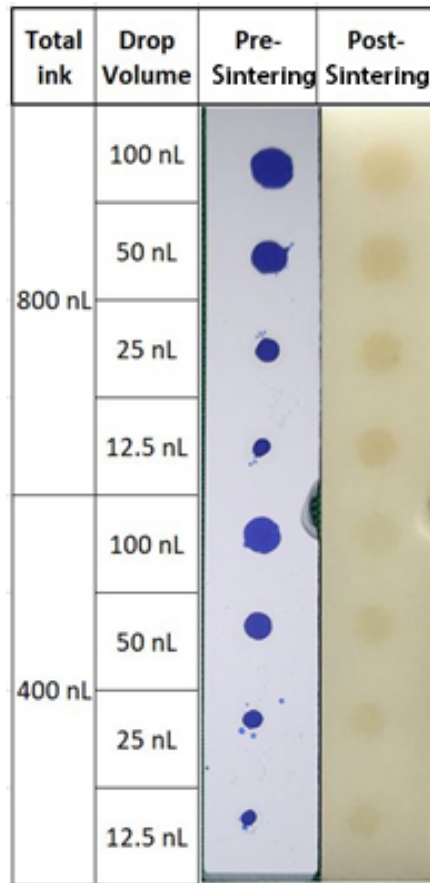
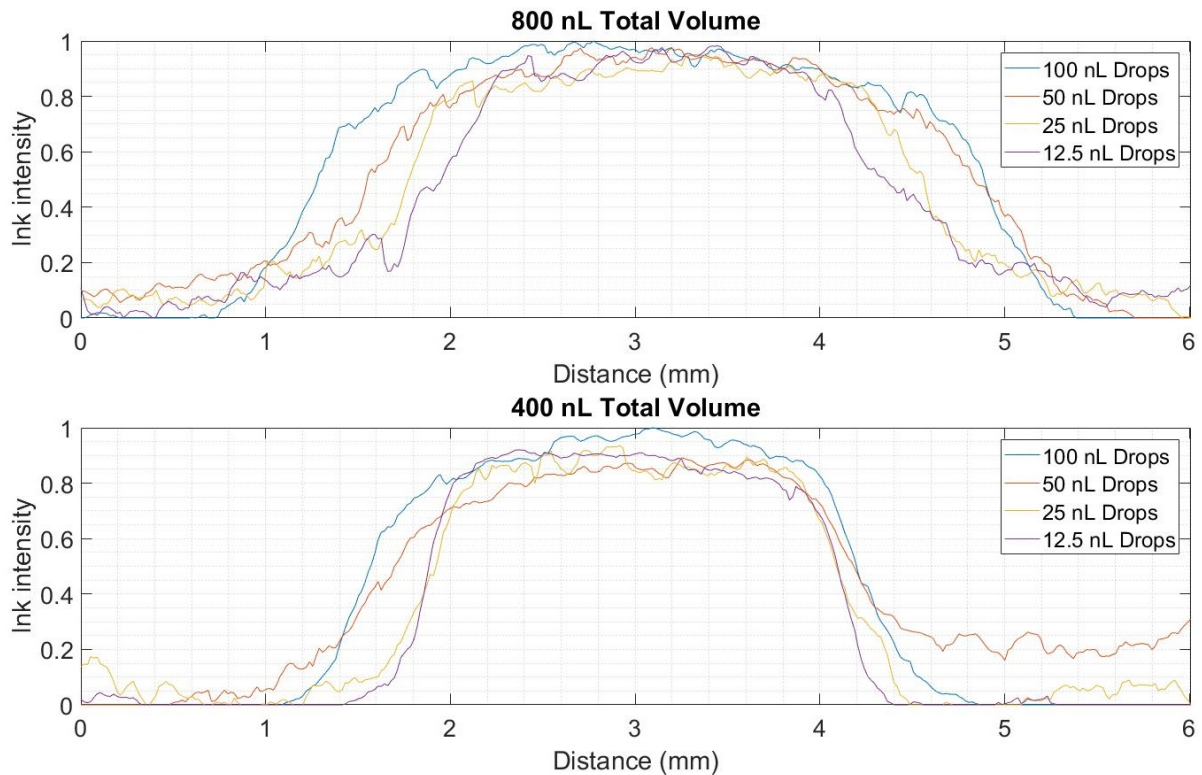


Figure 10.4: Effect of the drop size on the spot area

In the figure 10.4 one can see a printed zirconia specimen. Each spot on the upper half has a total ink volume of 800 nL and the ones on the bottom half 400 nL. These spots are printed using drops with volumes of 100, 50, 25 and 12.5 nL. The first image shows the spots right after printing. The second one shows the surface after furnacing.



*Figure 10.5: Comparison of the spot area results depending on the drop size*

The graphs show the ink intensity along the red lines and the spreading of the ink in lateral direction for each drop volume. 12.5 and 25 nL drops result in a similar spot diameter but the spots tend to get significantly larger with 50 and 100 nL Drops. Depending on these results 25nL can be selected as the optimum drop size for further experiments. However, considering to repeat some key procedures for the drop size of 50 nL can also be advantageous to gather further information.

## 10.4 Proximity

The proximity effect describes in the case of dental printing the coloring of the unprinted area between two printed areas proximate to each other. The closer the printed areas are, the saturated becomes the unprinted area in between.

If the color change of the unprinted area can be described depending on the ink concentration and distance between the printed areas, the effect of the proximity can be implemented to the model. During this experiment an exception is made and for the

printing process a drop size of 12.5 nL is chosen. This is the smallest volume the printing system can generate stably, without spraying the ink in a circle or generating satellite droplets. The reason for selecting the smallest possible droplet volume is to rule out or at least minimize the lateral flow of the ink caused by the initial wetting area.

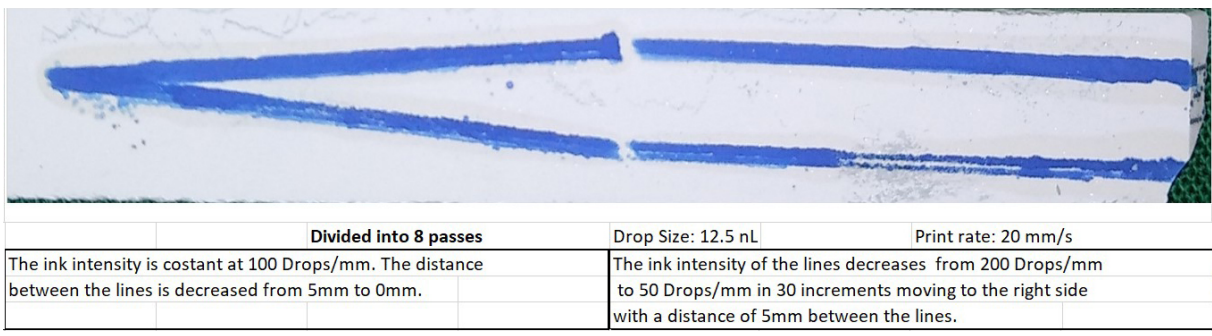


*Figure 10.6: Printed pattern for the proximity effect*

A pattern with varying distance between two lines and another pattern with varying droplet concentration were printed on the zirconia. The blue lines mark the initially printed surface portion before the sintering process, without taking the diffusion of the ink in the material into account. The dental ink is not easily recognizable by the naked eye before the sintering process, but it can diffuse far into the zirconia. The blue ink is added to the dental ink bottle to make the printed area recognizable. However, the blue ink cannot infiltrate the zirconia as good as the dental ink and gets filtered, gathering mostly on the initial contact area. If the Figure 10.6 is observed closely, one can recognize a slightly darker trace around the blue lines in comparison to the natural whiteness of the zirconia surface. The darker regions are infiltrated by the dental ink and seem to have a definite border. However, the sharp transition from the infiltrated to dry cannot be withheld after the sintering process.

The pattern on the left side presents two lines starting on the same coordinates and reaching a distance of 5 mm at right end. The ink trace has a constant concentration of 1250 nl/mm. The pattern on the right side presents two lines with a constant distance of 5mm to each other. On the left end of the lines, the ink intensity is 625 nl/mm and reaches linearly 2500 nl/mm towards the right end of the pattern in 30 incremental steps.

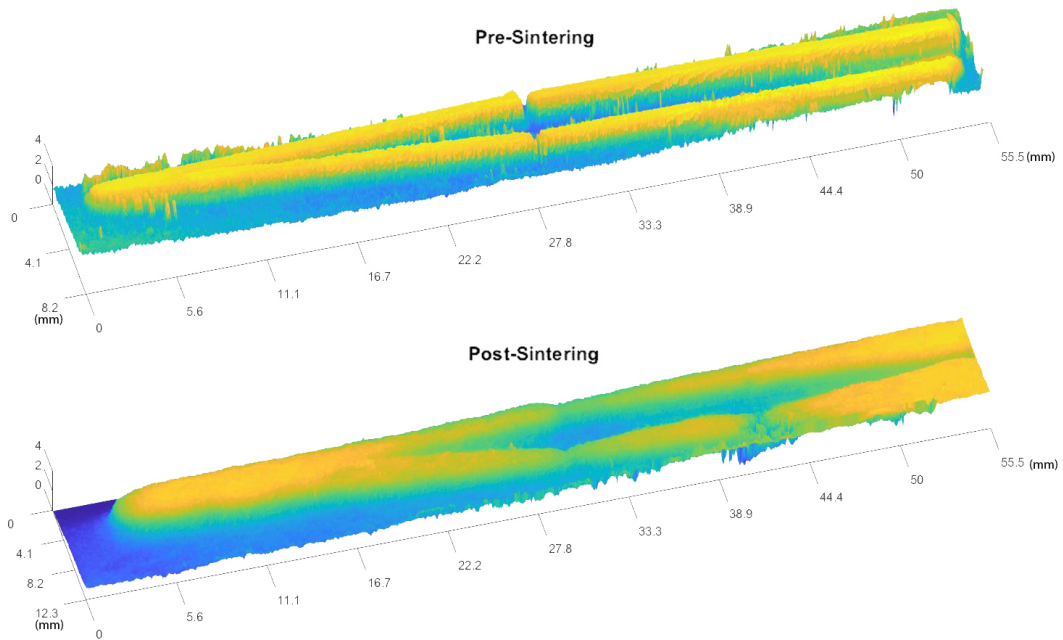


*Figure 10.7: Ink intensity analysis of the printed pattern before and after the sintering process*

Observing the Figure 10.7, one can qualitatively conclude, that the proximity has a significant effect on the coloring behavior. More than a half of the pattern seems to be one thick line on the left side of the postsintering graph in contrary to the lines recognized in the presintering analysis graph.

The second pattern with the varying ink intensity contains a flaw. The lower line is weaker in the middle because of a contamination with finger oil, which happened before the printing process. Nevertheless, the experiment was proceeded in order to observe, how seriously the printing process is affected by a slight finger oil contamination. The result shows a serious fluctuation in the acquired color which is as high as two shades.

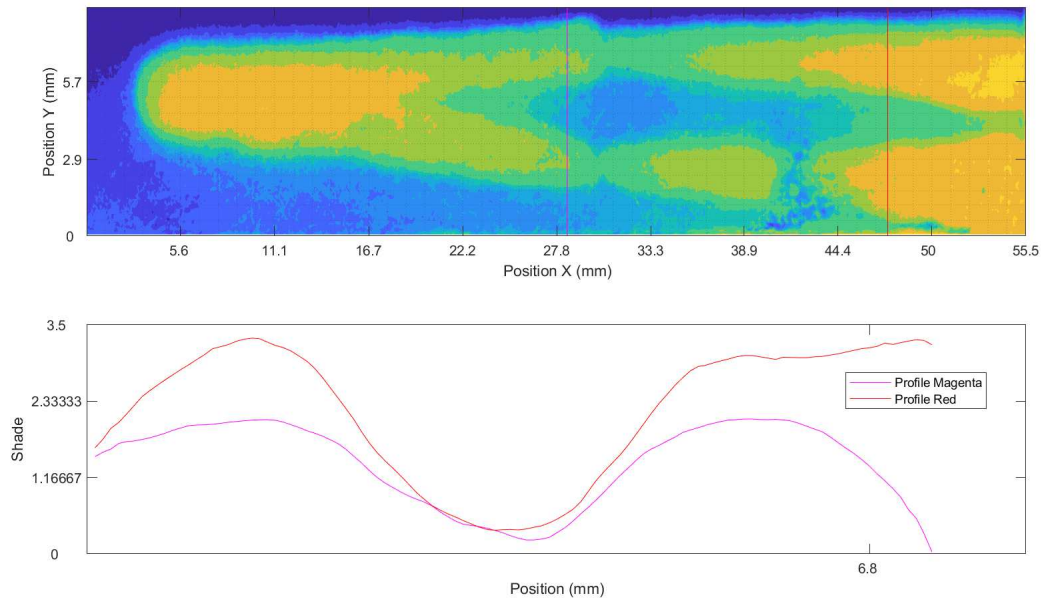


*Figure 10.8: Comparison of two profiles belonging to imprints with identical parameters*

The purpose of the experiment was to define the optimum trace distance for various ink intensities. The result of the first pattern is to be utilized to confirm the integrity of the results of the second pattern. The ink distribution on the line, where the distance between the two lines is 5 mm in the first pattern, magenta line in the Figure 10.8, should be the same with the ink distribution along the red line on the second pattern in the Figure 10.8 where the printing ink intensity is 1250 nL/mm. If the results would comply with each other, the optimum trace distance for any ink intensity could be calculated. However, the effect of the lateral diffusion was underestimated at time of planning the concept, which resulted with a divergent result that can be observed in the lower graph in the Figure 10.8. The ink diffusing from the higher intensity regions on the right side increase the intensity of the regions on the left side, so that the color intensity distributed over the red line does not belong to the printing intensity of 1250 nL/mm.

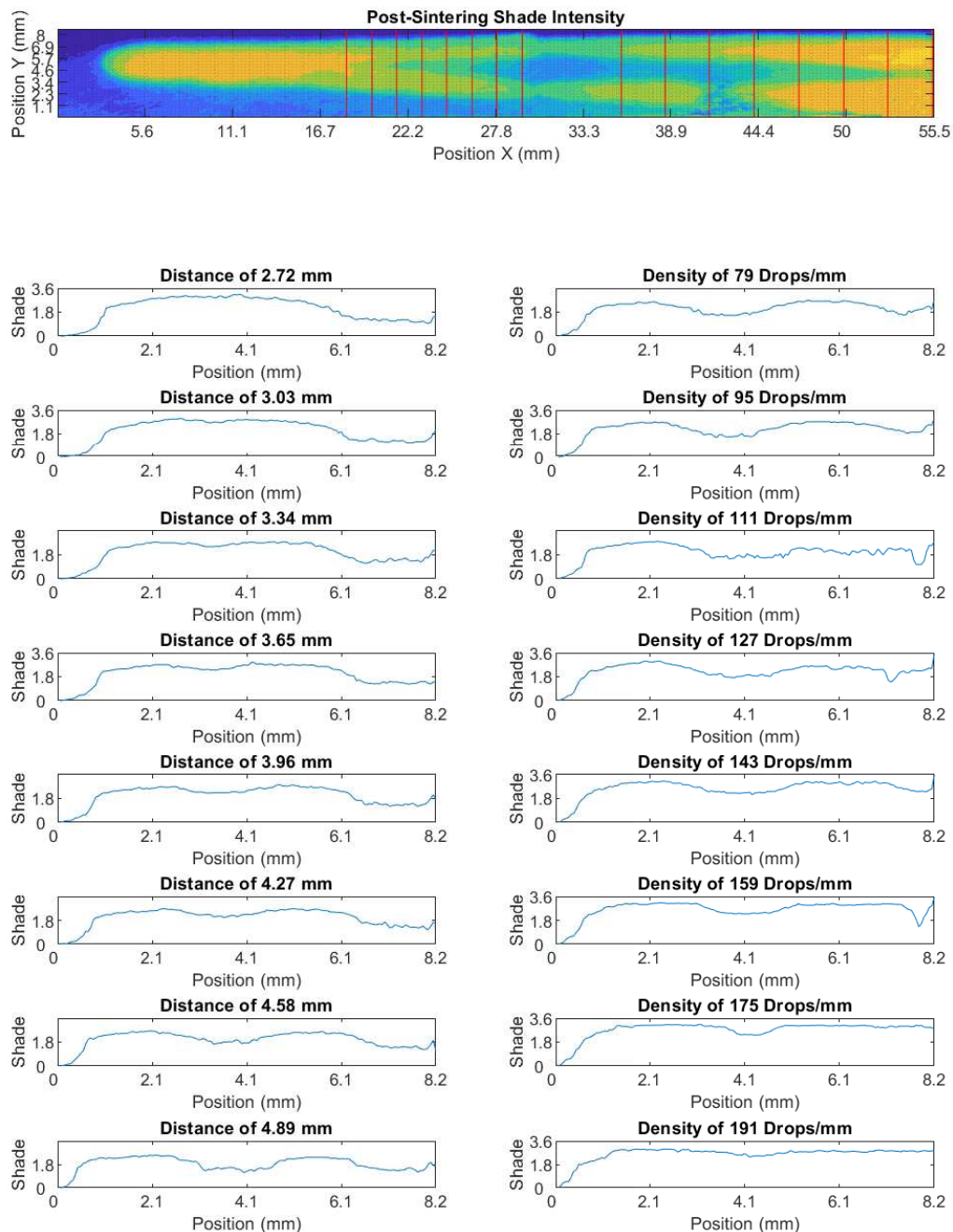


Figure 10.9: Profiles of color intensity depending on the distance on the left and depending on the ink amount on the right

The plots to analyze the ink distribution are presented separately in two columns in the Figure 10.9. The column on the left side presents 8 equidistant positions on the varying distance pattern which are marked with eight red vertical lines and the right column contains the cross section of the pattern on the right side with varying ink intensities. The pattern on the left shows that a necking appears already with a distance of 3 mm when the printing intensity is equal to 1250 nl/mm. In other words, printing with a trace distance higher than 3 mm result with an unwanted brighter stripe in the middle of printing traces. Whereas, a trace distance lower than 3mm cannot result with a more saturated color but a higher diffusion range or a thicker single line.

The data acquired from the first pattern was planned to be matched with the data from the section with the ink intensity of 1250 nl/mm on the second pattern but the extreme irregularity levels of diffusion in the x direction make the data acquired from the second pattern quite useless. Not to mention a direct match and acquisition approach, it is even not possible to calibrate the data on the second pattern to conduct trace distance calculations, because of the nonlinear lateral ink distribution inside the material along the second pattern.

## 10.5 Printing Angle

The dental crowns do not always present convex features. The chewing surface can rarely possess even some undercut geometries. In such cases, it is not possible for a droplet to land on the zirconia surface vertically and for some known areas, the printing process has to be conducted on skew surfaces.

If the lateral momentum of the droplets are high enough at the moment of the impact on the surface, the printed pattern can look like it has a motion blur effect. It is also possible that the resolution gets lower because of the lateral flow of the drops on the surface. There has to be some critical angle at which such disadvantages become inevitably significant. The maximum milling angle used for the dental crowns is declared by Bredent GmbH to be  $30^\circ$ . So, an experiment to test the effects of printing on a skew surface up to an angle of  $45^\circ$  is supposed to be comprehensive enough.



*Figure 10.10: Comparison of the spot area results depending on the drop size*

In order to test the effect of printing on a skew surface two parallel lines are printed on the surface which have a distance of 4 mm. This process is repeated 4 times, while the zirconia specimen was standing at angles  $0^\circ$ ,  $15^\circ$ ,  $30^\circ$  and  $45^\circ$ . The printed sample can be seen in the Figure 10.10. The highest possible printing angle that could be required is defined by the dental technologists from the Bredent GmbH to be  $30^\circ$  because of the traditional parameters of the milling process. The maximum milling angle for the inner features of the crown is realized by a CNC with a machine tool angle of  $30^\circ$  to the crown axis. So the extension of the experiments up to a printing angle of  $45^\circ$  is slightly off the limits but necessary to be on the safe side.

The lines were generated using 25 nL droplets with a drop density of 50 drops per mm. The thickness of the lines are measured as  $2.2 \pm 0.1$  mm. The measurements of the thicknesses as 2.2 mm on the specimen belong to the blue lines, which present the contact area on the zirconia with the ink. 2.2 mm is not the thickness of the lines after the sintering process. The consistency of the thicknesses at all angles is enough for the observer to draw the conclusion that the printing angles up to  $45^\circ$  do not cause any significant change in the printed pattern. If the wetted surface on the zirconia is the same for all of the printing angles, the possibility of observing different line properties after the sintering process is quite close to zero.

## 10.6 Singular Spot Characteristics

Since the efforts to determine the characteristics via continuous lines did not provide conclusive results because of the ink diffusion inside the porous material, discontinuous, isolated imprints are required as a further experiment. 8 Spots are to be printed with an equidistant placement. The distances between the spots are 8 mm which is beyond the diffusion range of the relative ink amounts. 25 nL drops and 50 nL drops are deployed on two different specimen to observe the effect of the droplet size depending on the total ink volume.

The drops are expected to have a high color intensity in the middle. That middle point is going to be the center of the Gaussian distribution. The points with an equal distance from the middle are supposed to present a point symmetrically identical color intensity.

Exp1									
Drop Volume	25	25	25	25	25	25	25	25	nL
Drop Count	8	16	32	48	64	80	96	112	-
Drop number	0.5	1	2	3	4	5	6	7	-
Multiplier									-
Passes	2	4	8	12	16	20	24	28	-
Total Ink Volume	200	400	800	1200	1600	2000	2400	2800	nL
Exp2									
Drop Volume	50	50	50	50	50	50	50	50	nL
Drop Count	4	8	16	24	32	40	48	56	-
Drop number	0.5	1	2	3	4	5	6	7	-
Multiplier									-
Passes	1	2	4	6	8	10	12	14	-
Total Ink Volume	200	400	800	1200	1600	2000	2400	2800	nL

Figure 10.11: Comparison of the spot areas depending on the drop size and total ink amount

The Figure 10.11 presents both of the printed zirconia plates before the sintering process combined with additional tables to sort the properties of each printed spot in a well defined manner.

In order to inspect the Gaussian distributions of the ink intensities in cases of different total ink amounts and different drop sizes 8 spots are printed using drops with volumes of 25 nL and 50 nL. The total ink volumes for the spots on each plate are identical and equal to 200 nL, 400 nL, 800 nL, 1200 nL, 1600 nL, 2000 nL, 2400 nL and 2800 nL. The lack of a color sampling device for shade measurement, channeled the color determination process to a software solution. The images captured with a standard camera are edited via MATLAB to acquire data about the color intensities. After the sintering process, the plates were laid on a homogeneous light source with a constant output level of 570 nits. The color distribution observed on the front side of the plates was captured using a high resolution camera. The captured image is processed utilizing the image processing toolbox of MATLAB. What important was, that the colors were not drifted out of scale during the editing processes which would make all of the results useless for further calculations. In order to increase the global contrast, histogram equalization

is conducted. The working principle of the histogram equalization process is similar to application of a band pass filter after an analysis is made with the Fourier transform. The intensities of different wavelengths in the image are analyzed. The interesting part of the wavelength spectrum is cropped and distributed over the whole visible spectrum conducting a linear scaling. This process makes it easier to distinguish between the slightest color changes. Then the image is converted from an RGB image to a gray scale one, since the intensities of the 3 colors are not individually relevant to the purpose of the experiment.

After this point, the darkness of each pixel presents its color intensity. Since the image contains a region which is printed beyond the maximum saturation level, a small pixel region with the highest intensity can be used for calibrations purposes as a dental shade of A3.5. The calibration shade is A3.5, because at the time of the development processes A3.5 is the most saturated shade provided by the research partner. Calibrating the other end of the spectrum for the lowest intensity is not such a straightforward calculation. Each line of the image actually has a slight different illumination because of the irregularities on the edges of the zirconia plate or even some defects on the plate like curved surfaces due to sintering process or broken regions.

One example to such defects can be observed in the Figure 10.12 on the false colored intensity image positioned on the left side. Just below the second spot from the top are lots of pixels contaminated with intensity noise. The reason for that is a crack in the plate, along the x-axis, at the position  $y=49$  mm. Since the wall of the plate at breaking line is not parallel to the XZ-Plane and does not have planar surface, the light guided into the material is not homogeneous either.

The calibration of the lowest intensity is made because of the mentioned reason separately for each line of the zirconia image. At each level it is known that the regions close to the edges of the zirconia plate contain no coloring agent. Edges of the plate are also illuminated with different intensities in comparison to the continuous regions in the middle. Thus, the minimum intensity value is obtained cutting out the regions close to the material border and taking the minimum intensity as a reference point for the shade A0.

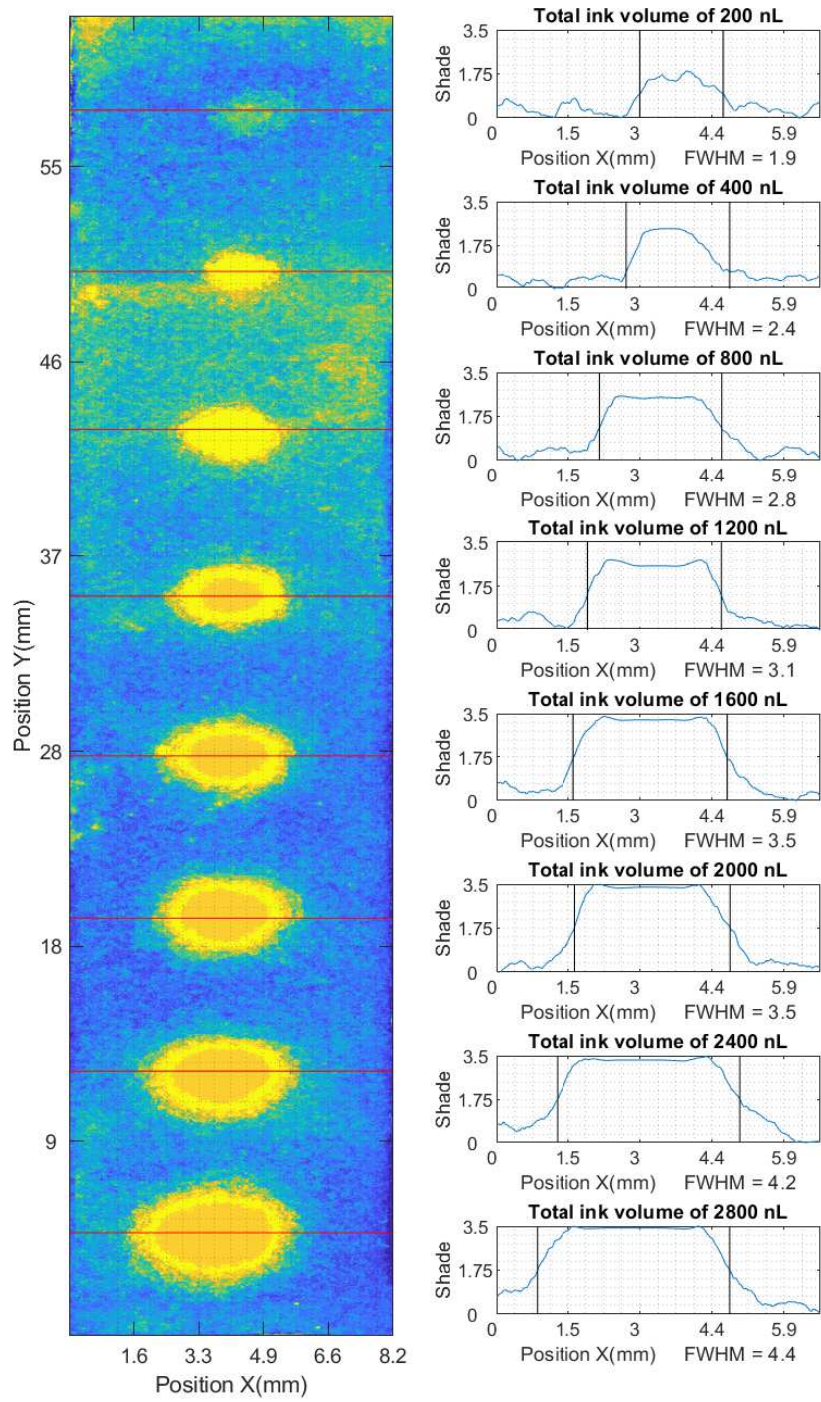


*Figure 10.12: False color representation and shade spreading analysis of the spots after sintering (printed with 25 nL drops)*

Due to the nonlinear printing characteristics of the porous zirconia medium, a proportional intensity change cannot be observed along increasing total ink amounts. As a reminder, it should be said that the printing process is realized using an ink with a calibrated shade of A3.5. This means if the zirconia plate is sunk into the ink completely and hold in the ink for at least 10 seconds so that there is relatively no air left in the porous medium, the end color shade of the zirconia would be an A3.5. This global void filling condition can also be fulfilled locally with the inevitable occurrence of some lateral diffusion.

There are two parameters one should pay attention to on the plots positioned on the right side of the Figure 10.12. One of them is the shade, the other one is the Full Width Half Maximum (FWHM) measurement of the spots. Each plot belongs to the line on the false colored image, on the same height with the plot. The applied amount of ink on the first spot is 200 nL. Even though the plot has a global maximum around A1.75, the results are not trustworthy, because of the noise level on the line. The areas close to the edges reach easily 50% of the global maximum which is a sign of low signal to noise ratio and is caused by extremely low amount of the applied ink.

The spots with total ink amounts of 1600 nL and 2000 nL present the same FWHM value which is equal to 3.5 mm. The 1600 nL total ink amount brings the graph just below the shade A3.5, but the total ink amount 2000 nL reaches the shade A3.5 with a constant level plateau. This means 2000 nL is the critical value for full saturation under lateral diffusion conditions. A higher amount of ink causes only a proportionally larger FWHM. For 25nL Drops it can be said that different shades can be obtained using an ink with the shade A4.0 and a brightener with a total amount of 2000 nL on each spot.

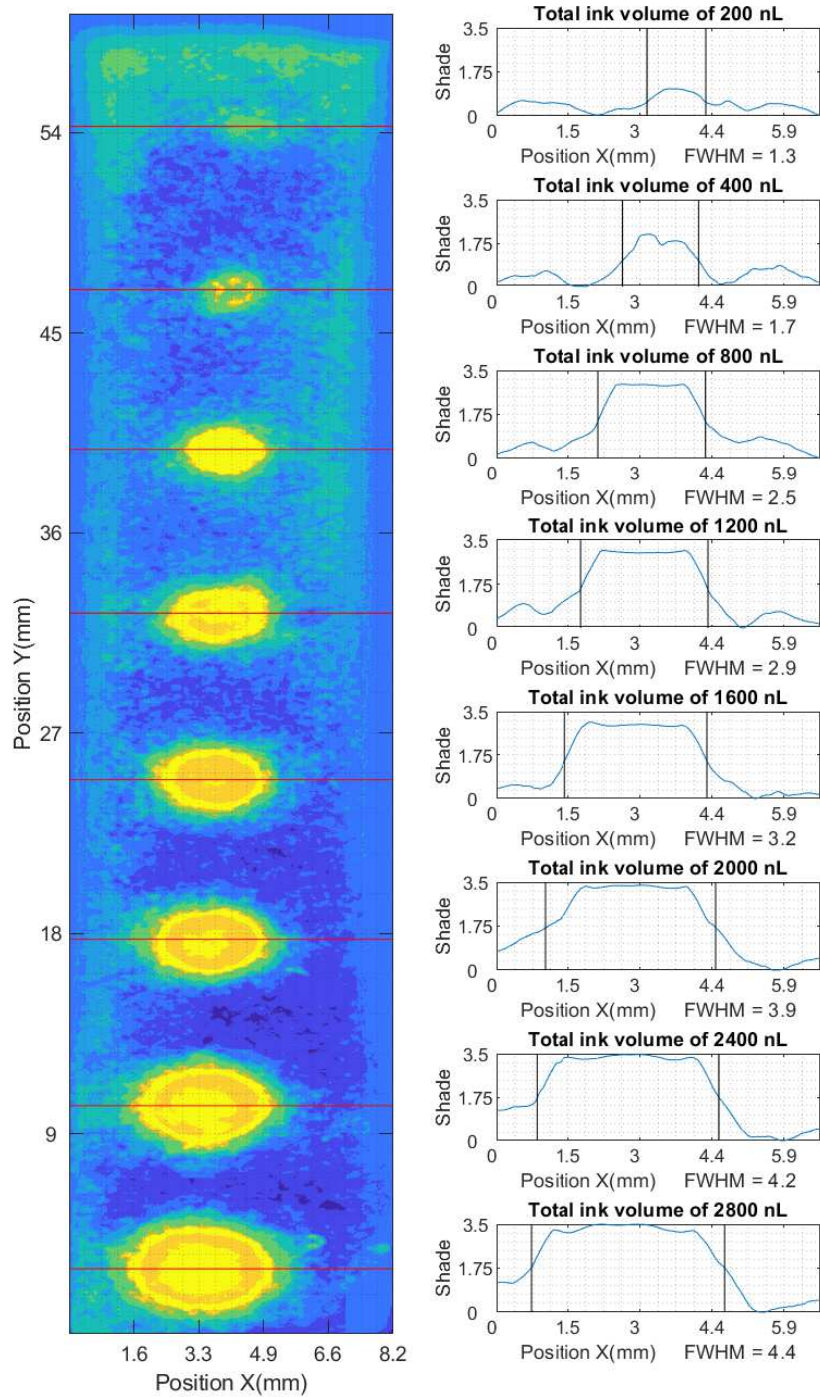


Figure 10.13: False color representation and shade spreading analysis of the spots after sintering (printed with 50 nL drops)

The same experiment is repeated for the drop size of 50 nL with the half amount of drops to achieve the same total ink amount. The only practical difference between the experiments is the diameter of the first contact circle. When the first wetting area is larger the ink tries to impregnate the zirconia through a larger area which means that the lateral diffusion is supposed to happen easier and the FWHM diameters are to be slightly larger than the ones belonging to the 25 nL droplets depending on the Equation 2.2 . It is hard to conduct a comparative evaluation for the first four spots from the top because of the high noise generated by the crack in the first specimen.

The spot created with 1600 nL ink has a lower shade level in comparison because of the higher diffusion distance of the ink caused by the larger initial contact. If the initial contact area is larger, the ink is transferred beneath this larger area into the zirconia material. After the impregnation the diffusion can happen beginning from a comparatively larger area which means that the ink can reach further away, but with less intensity. Since the ink is distributed more to the outer circles, the intensity of the 1600 nL spot is lower for 50 nL drops in comparison to 25 nL ones.

The total ink amount of 2000 nL is again enough for the full saturation of the pores. The predefined shade of A3.5 is reached with a large plateau as a sign for the saturated spot imprint with an FWHM of 3.9 mm. The FWHM values for the ink amounts 2000 nL, 2400nL and 2800 nL in the first experiment were, as it can be seen in Figure 10.12, 3.5 mm, 4.2 mm and 4.4 mm. Those values are 3.9 mm, 4.2 mm and 4.4 mm in the second experiment. The fact that the last two diameters are exactly the same for both of the drop sizes shows that an amount of total ink this high is significantly over the saturation limit of the spot area.

There is another important result one can conclude out of these two samples. If the printing process was done with a color shade of A4.0 and the target shade was A4.0 ,the whole void proportion of the material would have to be filled with the ink for the shade A4.0. Whether the drops have a volume of 25 nL or 50 nL doesn't change the fact that the material has to be filled up regionally and this will cause inevitable lateral diffusions. Thus it is not quite likely to obtain A4.0 spots as tiny as A1.0 spots using an ink with a shade of A4.0. Because in the upper plots of the Figures 10.12 and 10.13it can be observed that the spots have shades below A1.75 and the FWHM values are less than or equal to the half of the saturated A4.0 generating spot diameters.

## **11 Summary and Outlook**

The coloring process of the dental crowns based on the Zirconia ceramics is a necessity because of the plain white appearance of the material with a 49% translucency. The coloring process is realized through utilization of the metal-ionic inks. The sintering procedure binds the ceramic powder to provide a dental material with a high structural strength and also generates the color via oxidizing the metal-ionic at temperatures about 1200°C. Depending on the type of the ink classified by the groups of A, B, C and D, the color is defined and the concentration of the applied color determines the shade of the application area. Since the coloring process of the dental zirconia is not a two dimensional paint application process, but a 3 dimensional ink distribution problematic, due to the depth dependent luminescence of the dental problems, the digitalization of the procedure is not as simple as it is for a desktop printer.

If the subject is approached from the perspective of the current state of the technology and research, it can be said that the coloring process is a complete manual procedure. The ink is applied on the surface by the dental technologist via a brush. The printing of the zirconia with a dental ink utilizing microdrops is an uncharted area, but there is a good amount of research conducted in the fields of microdrop generation and absorption behavior of porous materials. Conclusive experiments are done by Starov et al. to formulate the absorption time and spreading distance of a deployed single ink drop, which have constructed the backbone of the mathematical aspect of this thesis.

Utilizing a 5 axis router, the drop deployment procedure is automated. As color reservoirs 4 ink bottles with the highest saturation levels of the colors A, B, C and D are used with a brightener to achieve the shades of each color. The system is utilized to conduct some experiments to develop a model for the printing process. Ink and ceramic properties like the ink viscosities and surface tensions are obtained, as well as the ceramic porosity. The inks have a higher viscosity than water, which helps to extinguish the satellite drops. The porosity of the zirconia is obtained to be 43%, which defines the volume to be filled with the ink and the brightener.

In summary, the printing speed can be accelerated with shorter absorption durations which are proved to decline 50% with a 60°C increase of the temperature. The other most important factor affecting the printing speed is the volume of a single drop. The most optimum drop volume is found out to be 25nL when the printing resolution is considered as the key factor. Printing experiments up to a distance of 20mm cause no significant quality variance. The printing measurement were replied at angles of 0° , 15° , 30° and 45° and result was the same. Printing quality was as good as 0° when the process was replied at 45° .The effect of proximity plays a significant role in the printing trace distance. For the ink intensity of 1250 nl/mm, which is approximately the fully saturated ink amount for the trace on the test sample, the optimum trace distance was observed to be 3mm. Afterwards the shade generation method is inspected in a discontinuous method rather than continuous lines to eliminate the effect of the neighboring regions with high ink amounts. For the 25 nL and 50 nL drop volumes a total ink amount of 2000 nL can be said to reach the aimed color intensity with inevitable lateral ink spreading. Charting of the color shade vs the ink amount is not an efficient approach to the shade generation process because of the different spreading ranges caused by different liquid amounts. The point oriented shade acquisition approach can be realized with interlayered deployment of brightener and ink until reaching the total liquid volume of 2000 nL. The brightener to ink ratios for target shade acquisition are yet to be analyzed in order to generate a model for the automated printing process. In the last experiment it was observed that smaller FWHM could only be observed with lower ink amount. It could be considered to generate inks for the printing purposes with higher saturation levels, in comparison to the inks on the market, especially for the printing process. Finally a model can be generated utilizing the point spread function analysis and optical dot gain phenomenon in association, in order to predestine the perceived color at the end of the sintering process.

## Bibliography

- Clarke, A., Blake, T., Carruthers, K. and Woodward, A. (2002): „Spreading and imbibition of liquid droplets on porous surfaces“. *Langmuir*, VI. 18(8) PP. 2980–2984.
- Denry, I. and Kelly, J. R. (2008): „State of the art of zirconia for dental applications“. *Dental materials*, VI. 24(3) PP. 299–307.
- Hapgood, K. P., Litster, J. D., Biggs, S. R. and Howes, T. (2002): „Drop penetration into porous powder beds“. *Journal of Colloid and Interface Science*, VI. 253(2) PP. 353–366.
- Hille, P. (2013): „ZWP Zahnarzt Wirtschaft Praxis“. URL <https://epaper.zwp-online.info/epaper/gim/zwp/2013/zwp0113/epaper/ausgabe.pdf>.
- IDS CAD (2016): „Chang's liquid brochure“. URL <https://www.idscad.com/wp-content/uploads/2016/11/liquid-brochure-1-1.pdf>.
- Lee, E. R. (2002): *Microdrop generation*, VI. 5. CRC press.
- Lee, J., Radu, A., Vontobel, P., Derome, D. and Carmeliet, J. (2016): „Absorption of impinging water droplet in porous stones“. *Journal of colloid and interface science*, VI. 471 PP. 59–70.
- Markicevic, B., Li, H., Sikorski, Y., Zand, A., Sanders, M. and Navaz, H. (2009): „Infiltration time and imprint shape of a sessile droplet imbibing porous medium“. *Journal of colloid and interface science*, VI. 336(2) PP. 698–706.
- Nguyen, N.-T. and Wereley, S. T. (2002): *Fundamentals and applications of microfluidics*. Artech house.
- Pecho, O. E., Ghinea, R., Ionescu, A. M., Cardona, J. C., Della Bona, A. and del Mar Pérez, M. (2015): „Optical behavior of dental zirconia and dentin analyzed by Kubelka–Munk theory“. *Dental Materials*, VI. 31(1) PP. 60–67.
- Rogers, G. L. (2015): „The point spread function and optical dot gain“. *Handbook of Digital Imaging*.

- Shah, K., Holloway, J. and Denry, I. (2008): „Effect of coloring with various metal oxides on the microstructure, color, and flexural strength of 3Y-TZP“. *Journal of Biomedical Materials Research Part B: Applied Biomaterials*, VI. 87(2) PP. 329–337.
- Shapling, W. (2014): *Principles and Practice of Esthetic Dentistry-E-Book: Essentials of Esthetic Dentistry*. Elsevier Health Sciences.
- Starov, V., Kosvintsev, S., Sobolev, V., Velarde, M. and Zhdanov, S. (2002a): „Spreading of liquid drops over saturated porous layers“. *Journal of colloid and interface science*, VI. 246(2) PP. 372–379.
- Starov, V., Zhdanov, S. and Velarde, M. (2002b): „Spreading of liquid drops over thick porous layers: complete wetting case“. *Langmuir*, VI. 18(25) PP. 9744–9750.
- VITA (2014): „Vita VMK Master, Working Instructions“. URL [https://mam.vita-zahnfabrik.com/portal/ecms\\_mdb\\_download.php?id=63578&sprache=en&fallback=de&rechtsraum=&cls\\_session\\_id=&neuste\\_version=1](https://mam.vita-zahnfabrik.com/portal/ecms_mdb_download.php?id=63578&sprache=en&fallback=de&rechtsraum=&cls_session_id=&neuste_version=1).
- Zirkonzahn GmbH (2018): „Zirkonzahn Brochure“. URL <http://zirkonzahn.com/assets/files/brochueren/DE-Broschuere-Die-Zirkonzahn-Schule-web.pdf>.

## Figure List

1.1	Single tooth replacement . . . . .	1
1.2	Vitapan shadeguide . . . . .	2
3.1	Cutout of a lab card (Shapling 2014) . . . . .	9
3.2	Making of dental implants (Zirkonzahn GmbH 2018) . . . . .	10
4.1	False colored crowns after manual brushing (Zirkonzahn GmbH 2018)	11
7.1	Solution Structure . . . . .	15
8.1	Solution Processes . . . . .	17
10.1	5 axis printer design for dental ink (Matthias Leininger, Bredent GmbH)	21
10.2	Ink Properties . . . . .	22
10.3	Effect of heat on the absorption time . . . . .	24
10.4	Effect of the drop size on the spot area . . . . .	25
10.5	Comparison of the spot area results depending on the drop size . . .	26
10.6	Printed pattern for the proximity effect . . . . .	27
10.7	Ink intensity analysis of the printed pattern before and after the sintering process . . . . .	28
10.8	Comparison of two profiles belonging to imprints with identical parameters . . . . .	29
10.9	Profiles of color intensity depending on the distance on the left and depending on the ink amount on the right . . . . .	30
10.10	Comparison of the spot area results depending on the drop size . . .	32
10.11	Comparison of the spot areas depending on the drop size and total ink amount . . . . .	33
10.12	False color representation and shade spreading analysis of the spots after sintering (printed with 25 nL drops) . . . . .	35
10.13	False color representation and shade spreading analysis of the spots after sintering (printed with 50 nL drops) . . . . .	37